acarbonyls. While transferance of $f_{MC,CO}$ to the M–CO linkages in $M(CO)_5(CS)$ is certainly reasonable, this may be a poor approximation for the M–CS linkages. Consequently the $f_{CS}$ and $f_{MC}$ values contain some uncertainty which cannot be removed given the present frequency data; $^{13}C$ substitution at the thiocarbonyl carbons is necessary to refine all the force constants in the M–CS linkages.

Contribution from the Department of Chemistry, Florida State University, Tallahassee, Florida 32306

# Lattice Effects on the Electron Resonance of Halopentaamminechromium(III) Complexes. Temperature Dependence

B. B. GARRETT* and M. T. HOLBROOK

*Received March 1, 1976* AIC601535

The spin-Hamiltonian parameters of $[Cr(NH_3)_5X]$ in $[Co(NH_3)_5X]Y_2$ hosts (X = Cl, Br; $Y^-$ = $Cl^-$, $Br^-$, $I^-$, $NO_3^-$) have been measured in the temperature range from 75 K to the decomposition temperature (430–550 K) and at 4 K. The nitrates show large changes near 130 K, while the halides have smooth variations over the entire temperature range. The implications of these data about the nature of lattice perturbations are discussed. Determination of the sign of the zero-field splitting from powder spectra is described.

## Introduction

The effects of nearest-neighbor counterions on the electron resonance spectra of halopentaamminechromium complexes were examined in a previous study.[1] It was shown that at least two separate mechanisms were necessary to account for the variations in the zero-field splitting tensors of $[Cr(NH_3)_5X]Y_2$ (X = Cl, Br; $Y^-$ = $Cl^-$, $Br^-$, $I^-$, $NO_3^-$) which were substituted into the isomorphous series of analogous cobalt hosts. The primary effect, a decrease of the axial parameter $D$ with increased counterion size, was attributed to a variation of the orientation of repulsive forces between the counterions and the bound halide, which protrudes through the face of the roughly eightfold cubic arrangement of counterions. This mechanism can be visualized by noting the relative positions of the halides in the $a$–$c$ projection of the orthorhombic unit cell of $[Co(NH_3)_5Cl]Cl_2$ shown in Figure 1. A larger counterion would be less effective in pushing the bound halide away from the metal, thereby leaving a more nearly cubic field at the metal site; thus the axial parameter, $D$, is smaller for larger counterions. A logical consequence of this mechanism would be a similar decrease in $D$ with an increase in temperature because the larger thermal motions of the counterions will give a smaller average repulsion of the bound halide. This contrasts with an earlier observation that there was no difference in the EPR spectra at 77 and 300 K for $[Cr(NH_3)_5Cl]Cl_2$ in the analogous cobalt host.[2] But that observation was accidental as we shall see from the full temperature dependence of the spectra.

The second mechanism, which was associated with variations of the rhombic zero-field splitting parameter $E$, was not so well characterized in our counterion dependence study.[1] It was observed that $E$ is larger with chloride and iodide counterions than with bromide and nitrate counterions, but no explanation was found. The $[Co(NH_3)_5Cl]Cl_2$ host is measurably nonaxial at the cobalt site as seen from the positions[3] and thermal ellipsoids of the nitrogen atoms in the crystal lattice.[1] The quadrupole asymmetry parameter $\eta = 0.25$ for $^{59}Co$ in this lattice[4] has a larger nonaxiallity than the chromium guest which has an analogous EPR asymmetry parameter $3E/D = 0.15$. Since no intramolecular origin for $E$ exists, the rhombic parameter $E$ is entirely of lattice origin and shows a large variation with the nature of the counterion. As with the axial parameter, the temperature dependence may be useful in elucidating the origin of the rhombic parameter in these systems.

There have been a number of studies[4–11] on lattice motions in amminecobalt complexes using nuclear resonance of protons, deuterons, and chlorine and cobalt nuclei, and these motions may have some bearing on the temperature variations of the electron resonances studied here. These studies have shown that threefold rotations of the ammines usually persist even at liquid nitrogen temperature unless some specific hydrogen-bonding interaction restricts the process.[5–9] Whole complex ion rotations can begin above 200 K provided that the motion does not interchange ammine ligands with halogen ligands. Such whole ion motions have been observed[5,7,8] for $[Co(NH_3)_6]^{3+}$, $[Co(NH_3)_5H_2O]^{3+}$, and *trans*-$[Co(NH_3)_4Cl_2]^+$ but not for *cis*-$[Co(NH_3)_4Cl_2]$.[10,11] Surprisingly, whole ion motions have not been observed for $[Co(NH_3)_5X]Y_2$; $[Co(NH_3)_5Cl]Br_2$ and $[Co(NH_3)_5Br]Br_2$ exhibit only the threefold ammine rotations over the range from 110 to 350 K.[6] Thus, in the host lattices used in the present study and presumably for the guest chromium complexes as well, the ammine ligands are undergoing rotations about the bond axis which are sufficiently fast to average the proton dipole–dipole interaction. It is also notable that at ambient temperatures the bound chlorine quadrupole resonance was not observable in $[Co(NH_3)_5Cl]Cl_2$ even though the cobalt resonances were seen, while both types of resonance were seen under similar conditions in the $[Co(NH_3)_5Cl]SO_4 \cdot H_2SO_4$.[4] This indicates an unusual relaxation time which may be associated with contact repulsions.

## Methods and Results

Starting materials $[Cr(NH_3)_5Cl]Cl_2$, $[Cr(NH_3)_5Br]Br_2$, and $[Co(NH_3)_5Br]Br_2$ were made via standard preparations involving the heating of the aquopentaammine or carbonatopentaammine complexes in the presence of HCl or HBr.[12–14] $[Co(NH_3)_5Cl]Cl_2$ was obtained commercially and recrystallized several times from a minimum amount of water. Each compound was ground with cold concentrated $H_2SO_4$ until HCl or HBr ceased to evolve. The very soluble sulfate or bisulfate salt of the complex was dissolved in water and reprecipitated with excess $H_2SO_4$. Mixed crystals were obtained by dissolving about 0.006 g of the chromium salt with about 0.3 g of the cobalt salt in 50 ml of water in an ice bath and saturating the solution with the sodium or potassium salt of the desired counterion. Dry air was then passed over the 0 °C solution for approximately 24 h. The crystals were filtered, washed with ethanol and ether, and allowed to air-dry before being ground into a very fine powder for placement in

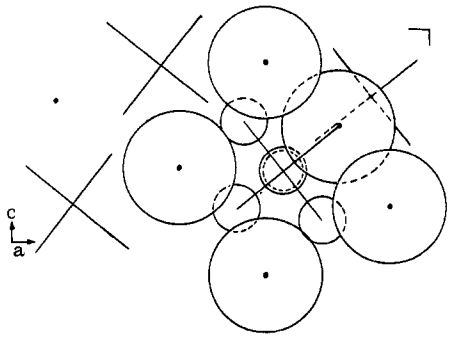


**Figure 1.** An $a$–$c$ projection of $[Co(NH_3)_5Cl]Cl_2$ with one molecular ion and its nearest neighbors shown as spheres of the appropriate van der Waals radius. The nearest neighbors form a distorted eightfold cube with the four chlorides shown above the body-centered complex and four more chlorides directly below.

quartz capillary tubes. Samples obtained in this way gave excellent powder EPR spectra with sufficiently narrow lines that the peaks and baseline crossings could be reproducibly measured within a few tenths of 1 G. There was no indication of foreign ions in the immediate vicinity of the paramagnetic guest which would give impurity spectra[15] nor was there evidence for paramagnetic impurities which give a very broad wave in the center of the spectra.[2,16] Samples of $[Co(NH_3)_5Br]I_2$ hosts were prepared as in a previous study.[1] Spectra of this sample were of much poorer quality than the others, which is reflected by the scatter in the plots of $D$ and $E$ vs. temperature.

Powder electron resonance spectra were obtained, assigned,[16] and fitted[1,15] by complete diagonalization at each resonant magnetic field of a spin Hamiltonian of the form

$$\mathcal{H} = \beta H \cdot g \cdot S + D'[S_z^2 - S(S+1)/3] + E'[S_x^2 + S_y^2]$$

The zero-field splittings will be described in units of gauss ($D$ (gauss) $= D'/g_z\beta$, $E$ (gauss) $= E'/g_\perp\beta$) because this allows the experimental frequency uncertainties (which were encountered at the extremes of the temperature range) to be absorbed in variations of the fitted $g$ factors. The $g$ factors of these samples were reported earlier[1] and no significant temperature dependence was seen in this study. Thus reporting the zero-field parameters in gauss gives the most direct measure of temperature-dependent lattice effects. The zero-field parameters observed here are in good agreement with the previously reported 35-GHz data[1] considering the change to X-band frequencies which was necessary to facilitate temperature variations.

Liquid helium temperature spectra of the $[Cr(NH_3)_5Cl]Y_2$ systems were taken at the University of Wyoming on a Varian E3 spectrometer at 9 GHz. Since the spectra at this temperature were quite broad, only qualitative results could be obtained. The values of $D$ are essentially what one would get by extrapolating the higher temperature data to liquid helium temperature. The values of $E$ for all 4-K spectra were approximately 40 G. This is somewhat surprising since at higher temperatures $E$ is quite distinctive. The sign of $D$ for $[Cr:Co(NH_3)_5Cl]Cl_2$ was determined to be negative from the relative intensities of the 4- and 77-K spectra. This measurement is less straightforward with powder spectra than it is with single-crystal data because of the differing intensities of low-field and high-field wing lines in powders. Low-field transitions tend to be pushed toward higher fields by perturbation mixing, which means that more orientations (angles) contribute to the low-field powder lines. Thus, we compared the relative intensities of the low- and high-field lines for 77- and 4-K data to determine that the low-field parallel line and high-field perpendicular line were enhanced at low temperature

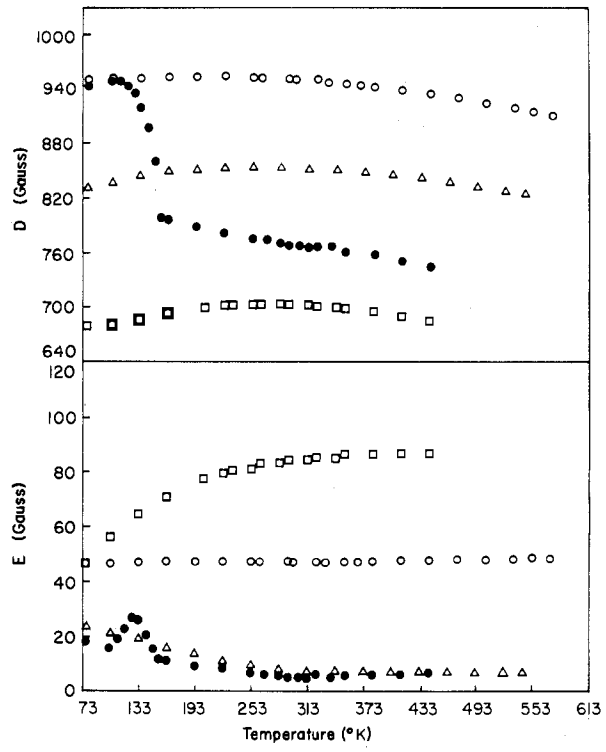


**Figure 2.** Temperature dependence of axial, $D$, and rhombic, $E$, zero-field splitting parameters for $[Cr(NH_3)_5Cl]$ in $[Co(NH_3)_5Cl]Y_2$ hosts. $Y^- = Cl^-$ (○), $Br^-$ (△), $I^-$ (□), and $NO_3^-$ (●).

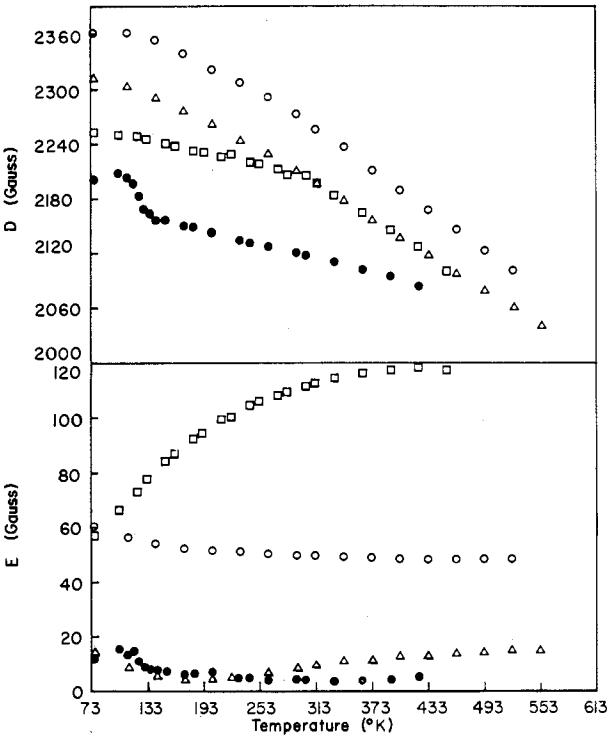


**Figure 3.** Temperature dependence of the zero-field splitting parameters for $[Cr(NH_3)_5Br]$ in $[Co(NH_3)_5Br]Y_2$ hosts. $Y^- = Cl^-$ (○), $Br^-$ (△), $I^-$ (□), and $NO_3^-$ (●).

implying that $D$ is negative. We were unable to make such determinations in three of the four samples examined because of badly broadened lines, overlap of the low-field line with double-quantum transitions, or weak signals on a rapidly varying baseline.

The temperature dependences of the zero-field splitting parameters $D$ and $E$ for the compounds $[Cr(NH_3)_5X]Y_2$ are

shown in Figures 2 and 3 where data for different hosts are plotted together for easy comparison. A complete tabulation of the spin-Hamiltonian parameters is given elsewhere.[17] The temperatures range from 77 K to just below the decomposition temperature of the host. The axial parameters of the $[Cr(NH_3)_5Cl]Y_2$ compounds exhibit only a small temperature dependence compared to those of the $[Cr(NH_3)_5Br]Y_2$ series. In accordance with the trend noted previously,[1] the magnitude of $D$ is smaller for larger counterions at any given temperature. The counterion rather than the complex appears to have more influence on the value of the rhombic parameter. The bromides and nitrates give essentially axial systems, while the chlorides and the iodides give asymmetric systems at all temperatures. For a given counterion the temperature dependence is very similar for both complexes. The bromides and nitrates give a rhombic parameter which decreases from a low value at 77 K to an even lower value at elevated temperature. The chlorides give an $E$ of approximately 50 G which is remarkably temperature independent. The rhombic parameter for the iodides increases to a relatively large value at high temperatures.

## Discussion

The temperature dependences of the chloropentaammine and bromopentaammine complexes are remarkably similar for each counterion. The axial parameters all have a nearly linear decrease at high temperature, although the chloro halides have some curvature even at the highest temperatures. The chloro complexes all show some increase of $D$ with temperature at lower temperatures. This gives peak values of $D$ near −50, −20, and 10 °C for chloride, bromide, and iodide counterions, respectively. This results in the $[Cr{:}Co(NH_3)_5Cl]Cl_2$ system having nearly identical spectra at room temperature and liquid nitrogen temperature and accounts for an earlier failure to recognize the existence of temperature-dependent lattice effects.[2] Our measurements do not extend to sufficiently low temperatures to observe any significant rise in $D$ for the bromo complexes, but the shapes of the curves are similar to those for the chloro complexes. The shapes of the rhombic parameter, $E$, curves are remarkably alike for both chloro and bromo complexes while showing a unique behavior for each counterion. Contrasting this, $E$ is about 40 G at 4 K for each of the four counterions with the chloro complexes. The chloride counterions give remarkably temperature-independent values of $E$ with that of the chloro chloride varying by only 2 G (47 to 49 G) from 103 to 573 K. But all of the rhombic parameters become relatively constant at high temperatures, which seems to contradict the obvious lattice dependence.

Perhaps the most striking phenomena illustrated in the temperature-dependence curves are the sharp breaks near 130 K in both $D$ and $E$ for the nitrate counterions. A plausible explanation of this break can be made if the nitrate ions are not rotating at low temperatures and behave as small counterions as far as the metal complex is concerned. At the transition temperature the ions begin to tumble and appear as larger ions. The effectively larger counterion would allow the bound halogen to relax into the face of the counterion cube (see Figure 1). The reduction in the metal–halogen bond length increases the ligand field along this axis causing a decrease in the axial parameter. Concomitant with this is a change in the rhombic parameter occurring over the same transition temperature range. However, instead of a monotonic change as in $D$, the value of $E$ rises to a peak and then decreases. There is no net change in $E$ other than that expected by the curvature of the data outside this range. This behavior indicates that during the change responsible for decreasing the axial parameter (presumably the onset of nitrate ion tumbling) there is an additional rhombic contribution, but both high- and low-temperature regions appear to have the same dominant $E$ mechanism.

Another possible explanation for the break in the zero-field parameters of the nitrate salts is that this feature might be an observation of the onset of ammine rotation rather than nitrate tumbling. The failure to observe such changes in the halide salts would then be attributed to stronger hydrogen bonding with the nitrate oxygen (and possibly better steric arrangements) preventing the onset of rotation until higher temperatures are reached. This alternative is not attractive because the liquid helium temperature data suggest that no such transition takes place in the halide salts and large differences in $E$ should exist above and below the transition which is not the case for the chloro nitrate system. The onset of ammine rotations would not explain the large decrease in $D$ either.

Previously, it was found that changes in the size of the counterion give a corresponding change in the lattice dimensions.[1] In other words, substituting a larger counterion into the lattice caused it to expand. Two mechanisms were necessary to explain the effect of this expansion on the zero-field splitting parameters. These same two mechanisms should also account for variations of zero-field splittings due to expansions caused by increases in temperature. The first mechanism involves the four counterions adjacent to the bound halide. As they move apart with increasing temperature, the bound halide which protrudes through the plane of these counterions can relax back toward the metal ion. This shortening of the bond will cause a decrease in $D$ with increasing temperature. A small contribution to $D$ can be made by the rhombic mechanism, and this change can be of either sign, depending on whether $E$ is positive or negative. The temperature dependence of the rhombic parameter shows no correlation with the axial parameter; thus, the rhombic mechanism appears to have a separate and independent response to lattice variations.

Bayer[18] and Kushida[19] developed a model to describe the thermal averaging of the quadrupole coupling tensor in crystals. While this model is usually developed in terms of the foreshortening of the laboratory frame or crystal frame projection of a tensor tied to the molecular frame of a torsionally oscillating molecule, it can also include the effects of stretching vibrations. This model can also describe the thermal averaging of any tensor tied to a molecular framework in a crystal such as the anisotropic **g** tensor, chemical shift tensor, or the zero-field splitting tensor. The model predicts a falloff of the tensor anisotropy from a low-temperature limit to a linear high-temperature region, where $kT$ is large relative to the energy of the averaging motion. Application of the Bayer–Kushida model to the high-temperature region for $D$ leads to estimates of torsional oscillation frequencies between 10 and 30 $cm^{-1}$ for the requisite averaging motions. These values are reasonable for molecular complexes of this size, but the model also requires a similar averaging of $E$ which is not observed in any of these systems. In addition, the thermal ellipsoids of the ligand motions appear to be channeled along the bond axes rather than torsionally.[1] The counterion repulsion mechanism gives the same high-temperature prediction as the Bayer–Kushida model and there is no evidence that the latter model makes any significant contribution to the lattice effects under consideration.

It appears more profitable to view the lattice effects as arising from the shape of the cavity into which the guest ion is placed. Specific distortions will arise when the sizes of guest and host overlap and a more general channeling of the guest ion motions to fit the cavity will prevail otherwise. The nonzero high-temperature limiting values of $E$ and the counterion specific behavior of the rhombic parameter seem to be in accord with this picture. The counterion repulsion of the bound

halide still appears to be the primary reason for the different axial splittings with different counterions and provides a reasonable explanation for the high-temperature behavior of *D*. A third lattice mechanism will be necessary to explain the increase observed for *D* at low temperatures.

**Acknowledgment.** We wish to thank Professor S. L. Holt of the University of Wyoming for the use of his facilities for obtaining low-temperature spectra.

**Registry No.** $[Co(NH_3)_5Cl]Cl_2$, 13859-51-3; $[Co(NH_3)_5Cl]Br_2$, 13601-43-9; $[Co(NH_3)_5Cl]I_2$, 57255-93-3; $[Co(NH_3)_5Cl](NO_3)_2$, 13842-33-6; $[Co(NH_3)_5Br]Cl_2$, 13601-38-2; $[Co(NH_3)_5Br]Br_2$, 14283-12-6; $[Co(NH_3)_5Br]I_2$, 14591-70-9; $[Co(NH_3)_5Br](NO_3)_2$, 21333-43-7; $[Cr(NH_3)_5Cl]$, 14482-76-9; $[Cr(NH_3)_5Br]$, 22289-65-2.

## References and Notes

(1) M. T. Holbrook and B. B. Garrett, *Inorg. Chem.*, **15**, 150 (1976).
(2) L. E. Mohrmann, Jr., and B. B. Garrett, *Inorg. Chem.*, **13**, 357 (1974).
(3) G. G. Messmer and E. L. Amma, *Acta Crystallogr., Sect. B*, **24**, 412 (1968).
(4) I. Watanabe, H. Tanaka, and A. Shimizu, *J. Chem. Phys.*, **52**, 4031 (1970).
(5) G. R. Murray, Jr., and J. S. Waugh, *J. Chem. Phys.*, **29**, 207 (1958).
(6) S. Hayashi, *Kogyo Kagaku Zasshi*, **68**, 1449 (1965).
(7) T. Ito and T. Chiba, *Bull. Chem. Soc. Jpn.*, **42**, 108 (1969).
(8) T. Ito, *Bull. Chem. Soc. Jpn.*, **45**, 3507 (1972).
(9) M. Okabe, Y. Arata, A. Yamasaki, and S. Fujiwara, *J. Phys. Soc. Jpn.*, **28**, 935 (1970).
(10) B. A. Dunell, M. D. Pachal, and S. E. Ulrich, *Can. J. Chem.*, **51**, 1107 (1973).
(11) S. E. Ulrich and B. A. Dunell, *Inorg. Nucl. Chem. Lett.*, **9**, 85 (1973).
(12) M. Mori, *Inorg. Synth.*, **5**, 131 (1957).
(13) E. Zinato, R. Lindholm, and A. W. Adamson, *J. Inorg. Nucl. Chem.*, **31**, 446 (1969).
(14) G. Schlessinger, "Inorganic Laboratory Preparations", Chemical Publishing Co., New York, N.Y., 1962, p 210.
(15) S. J. Baker and B. B. Garrett, *Inorg. Chem.*, **13**, 2683 (1974).
(16) L. E. Mohrmann, Jr., B. B. Garrett, and W. B. Lewis, *J. Chem. Phys.*, **52**, 535 (1970).
(17) M. T. Holbrook, Ph.D. Dissertation, Florida State University, Tallahassee, Fla., 1976.
(18) H. Bayer, *Z. Phys.*, **130**, 227 (1951).
(19) T. Kushida, *J. Sci. Hiroshima Univ., Ser. A: Math., Phys., Chem.*, **19**, 327 (1955).

Contribution No. 570 from the Charles F. Kettering Research Laboratory, Yellow Springs, Ohio 45387

# Synthesis of Mo(IV) and Mo(V) Complexes Using Oxo Abstraction by Phosphines. Mechanistic Implications

GRACE J.-J. CHEN, JOHN W. McDONALD,* and W. E. NEWTON

*Received May 14, 1976* AIC603551

The reactions of the Mo(VI) compounds $MoO_2L_2$ (L = $S_2CNR_2$, $S_2PR_2$, cysteinato methyl ester, acetylacetonato, 8-hydroxyquinolinato) with tertiary phosphines provides a convenient route to the Mo(V) species $Mo_2O_3L_4$ and in some cases (L = $S_2CNR_2$, $S_2PR_2$) to the Mo(IV) complexes $OMoL_2$. The extent of the reduction, i.e., to Mo(V) or Mo(IV), is rationalized in terms of the magnitude of the equilibrium constant for reaction of $OMoL_2$ (formed by oxo abstraction) with unreacted $MoO_2L_2$ to form $Mo_2O_3L_4$ which must dissociate to be reducible. Infrared and visible spectral properties are given for the new dithiophosphinato complexes prepared by this method.

It has been reported[1] that triphenylphosphine abstracts an oxo group from dioxobis(*N*,*N*-dialkyldithiocarbamato)molybdenum(VI) $[MoO_2(S_2(S_2CNR_2)_2]$ yielding $OMo(S_2CNR_2)_2$ and triphenylphosphine oxide. This reaction, together with the recently discovered[1,2] equilibrium (eq 1), was

$$Mo_2O_3(S_2CNR_2)_4 \rightleftarrows MoO_2(S_2CNR_2)_2 + OMo(S_2CNR_2)_2 \quad (1)$$

used in the design[1] of a system for the catalytic aerial oxidation of phosphines. Because of our continuing interest in the chemistry of oxomolybdenum species as possible models for molybdoenzymes,[2-5] we have utilized and extended this type of oxo abstraction reaction to provide a convenient method of synthesis for a variety of oxomolybdenum(V) and -(IV) complexes. This report describes the synthetic methods and gives data which provide insight into the mechanism of the reactions.

## Experimental Section

All reactions were carried out under an argon atmosphere using standard techniques. All solvents were dried over molecular sieves and degasses prior to use. The compounds $MoO_2(S_2CNR_2)_2$ (R = Me, Et, *n*-Pr), $MoO_2(ox)_2$ (ox = 8-hydroxyquinolinato), and $MoO_2$(cyst-OMe)$_2$ (cyst-OMe = cysteinato methyl ester) were synthesized by literature methods.[6-8]

Infrared spectra were recorded on a Beckman IR20A spectrophotometer and uv–visible spectra on a Cary 118C instrument. Elemental analyses for CHN were determined in this laboratory using either a Hewlett-Packard 185 or a Perkin-Elmer 240 instrument.

**Synthesis of Compounds. $MoO_2(acac)_2$.** The complex was prepared by a modification of the literature methods.[9,10] $(NH_4)_6Mo_7O_{24}\cdot 4H_2O$ (30.0 g) was dissolved in $H_2O$ (100 ml) and acetylacetone (acacH; 40 ml) was added. The pH of the solution was adjusted to 3.5 using 10% $HNO_3$ and a solid began to precipitate. After 1.5 h, yellow $MoO_2(acac)_2$ (28 g, 51% yield) (identified by ir spectrum) was isolated by filtration, washed with $H_2O$, ethanol, and ether, and dried in vacuo.

**$MoO_2(S_2PPh_2)_2$.** A solution of $HS_2PPh_2$ (4.0 g) in ethanol (50 ml) was added to a solution of $(NH_4)_6Mo_7O_{24}\cdot 4H_2O$ (1.5 g) in $H_2O$ (70 ml). After stirring for 20 min, yellow $MoO_2(S_2PPh_2)_2$ (2.54 g, 48% yield) was isolated by filtration, washed with $H_2O$, ethanol, and ether, and dried in vacuo. Anal. Calcd for $C_{24}H_{20}MoO_2P_2S_4$: C, 46.0; H, 3.22. Found: C, 46.3; H, 3.09.

**$MoO_2[S_2P(i\text{-}Pr)_2]_2$.** This compound was prepared in an identical manner to $MoO_2(S_2PPh_2)_2$. The yield was 5.10 g, 53%. Anal. Calcd for $C_{12}H_{28}MoO_2P_2S_4$: C, 29.38; H, 5.75. Found: C, 29.53; H, 5.87.

**$Mo_2O_3(acac)_4$.** $PPh_2Et$ (0.90 ml) was added to a solution of $MoO_2(acac)_2$ (1.0 g) in dichloroethane (50 ml) and the solution was refluxed for 45 min. The reaction mixture was cooled and the dark precipitate of $Mo_2O_3(acac)_4\cdot C_2H_4Cl_2$ (0.70 g, 72% yield) was isolated by filtration, washed with ethanol and ether, and dried in vacuo. Anal. Calcd for $C_{22}H_{32}Cl_2Mo_2O_{11}$: C, 35.9; H, 4.35. Found: C, 35.4; H, 4.12.

**$Mo_2O_3(ox)_4$.** $PPh_2Et$ (1.5 ml) was added to a suspension of $MoO_2(ox)_2$ (1.0 g) in dichloroethane (60 ml) and the reaction mixture was refluxed for 3.5 h. The dark precipitate of $Mo_2O_3(ox)_4$ (0.90 g, 92% yield) (identified by its ir and visible spectra) was isolated by filtration, washed with ethanol and ether, and dried in vacuo. Anal. Calcd for $C_{36}H_{24}N_4Mo_2O_7$: C, 52.9; H, 2.94; N, 6.86. Found: C, 52.3; H, 2.94; N, 6.55.

**$Mo_2O_3$(cyst-OMe)$_4$.** $PPh_3$ (0.86 g) was added to a suspension of $MoO_2$(cyst-OMe)$_2$ (1.0 g) in $CH_2Cl_2$ (50 ml). The reaction mixture was refluxed for 18 h, cooled to room temperature, and filtered, and the filtrate was evaporated to dryness under vacuum to yield a purple oil. Trituration with ethanol yielded the purple product (0.65 g, 67% yield), which was isolated by filtration, washed with ethanol and ether, and dried in vacuo. Anal. Calcd for $C_{16}H_{32}Mo_2N_4O_{11}S_4$: C, 24.7; H, 4.10; N, 7.22. Found: C, 25.0; H, 4.20; N, 7.00.

**$Mo_2O_3[S_2PPh_2]_4$.** $PPh_2Et$ (0.084 g) was added to a solution of $MoO_2(S_2PPh_2)_2$ (0.475 g) in $CH_2Cl_2$ (30 ml). The reaction mixture